

# A Study of the Coronal Plasma in RS CVn binary systems

M. Audard<sup>1</sup>, M. Güdel<sup>1</sup>, A. Sres<sup>1,2</sup>, R. Mewe<sup>3</sup>, A. J. J. Raassen<sup>3,4</sup>, E. Behar<sup>5</sup>, C. R. Foley<sup>6</sup>, R. L. J. van der Meer<sup>3</sup>

**Abstract.** *XMM-Newton* has been performing comprehensive studies of X-ray bright RS CVn binaries in its Calibration and Guaranteed Time programs. We present results from ongoing investigations in the context of a systematic study of coronal emission from RS CVns. We concentrate in this paper on coronal abundances and investigate the abundance pattern in RS CVn binaries as a function of activity and average temperature. A transition from an Inverse First Ionization Potential (FIP) effect towards an absence of a clear trend is found in intermediately active RS CVn systems. This scheme corresponds well into the long-term evolution from an IFIP to a FIP effect found in solar analogs. We further study variations in the elemental abundances during a large flare.

## 1. Introduction

The RS CVn binary system class is loosely defined as consisting of a chromospherically active evolved star orbiting within a few days around a main-sequence or subgiant companion (Hall 1976). Their short rotation period implies high levels of activity (e.g., Noyes et al. 1984), observed as strong emission of chromospheric lines and saturated X-ray emission (Dempsey et al. 1993). The high-resolution X-ray spectra of the brightest and nearby RS CVn binary systems obtained by *XMM-Newton* are well-exposed and provide a high signal-to-noise ratio. Abundant coronal elements (C, N, O, Ne, Mg, Si, S, Ar, Ca, Fe, and Ni) produce a rich spectrum of electronic transitions in the EUV and X-rays, allowing us to perform benchmark studies of atomic databases. Recent results with *Chandra* and *XMM-Newton* show that models reproduce the observed spectra fairly well (e.g., Audard et al. 2001a, Behar, Cottam, & Kahn 2001), although a significant number of lines, mainly from Si, S, Ar, and Ca L-shell lines, are either absent in the atomic databases or are not properly reproduced (Audard et al. 2001a). In this study, we have therefore discarded wavelength ranges where

---

<sup>1</sup>Paul Scherrer Institut, CH

<sup>2</sup>Institute of Astronomy, ETHZ, CH

<sup>3</sup>Space Research Organization of the Netherlands, NL

<sup>4</sup>Astronomical Institute “Anton Pannekoek”, NL

<sup>5</sup>Columbia Astrophysics Laboratory, USA

<sup>6</sup>Mullard Space Science Laboratory, UK

such lines dominate in order not to bias the convergence of the spectral fits, and especially to get more accurate elemental abundances.

Past stellar coronal abundance determinations have been done with CCD spectra of moderate spectral resolution (e.g., Drake 1996, Güdel et al. 1999) or with low sensitivity spectrometers (e.g., Drake, Laming, & Widing 1995, Laming, Drake, & Widing 1996, Schmitt et al. 1996, Drake, Laming, & Widing 1997). Abundance studies of stellar coronae are a powerful means to better understand the well-studied, but still puzzling, abundance pattern in the Sun: in brief, the solar corona and the solar wind display a so-called “First Ionization Potential” (FIP) effect, for which the current consensus is that the abundances of low-FIP ( $< 10$  eV) elements are *enhanced* relative to their respective photospheric abundance, while the abundances of high-FIP ( $> 10$  eV) elements are photospheric (e.g., Haisch, Saba, & Meyer 1996). Stellar coronal spectra often showed a metal abundance deficiency relative to the *solar* photospheric abundances (Schmitt et al. 1996), with  $\text{Fe}/\text{Fe}_\odot \approx 0.1 - 0.2$  in active RS CVn binary systems. More detailed studies with *EUVE* showed either the absence of any FIP-related bias (Drake et al. 1995), or the presence of a FIP effect in inactive stellar coronae (Drake et al. 1997). The current generation of X-ray observatories, *XMM-Newton* and *Chandra*, combine high spectral resolution with moderate effective areas to routinely obtain excellent data to measure abundances in stellar coronae.

An analysis of a deep exposure of the *XMM-Newton* RGS spectrum (Brinkman et al. 2001) of the RS CVn binary system HR 1099 showed a trend towards enhanced high-FIP elemental abundances (normalized to O and relative to the solar photospheric abundances, Anders & Grevesse 1989), while low-FIP elemental abundances were depleted; this effect was dubbed the “Inverse FIP” effect. Different active stars also show such a trend (Güdel et al. 2001ab), while the intermediately active binary Capella displays neither a FIP nor an IFIP effect (Audard et al. 2001a). It is practice to normalize stellar coronal abundances to the *solar* photospheric abundances, while they should better be normalized to the *stellar* photospheric abundances. The latter are, however, hard to measure due to enhanced chromospheric activity, high rotation rate and the presence of spots in active stars, particularly in RS CVn binaries. Nevertheless, for some stars, photospheric abundances are known. Güdel et al. (2002; also in these proceedings) discuss the transition from an inverse FIP effect to a “normal” FIP effect in the long-term coronal evolution from active to inactive solar analogs; all targets have photospheric abundances indistinguishable from those of the Sun, which suggests that the observed transition is real.

While low-FIP elements appear underabundant in the quiescent state, a notable increase of the abundances of “metals” during flares is often observed (e.g., Ottmann & Schmitt 1996, Favata et al. 2000). More precisely, time-dependent spectroscopy of a large flare in UX Ari (Güdel et al. 1999) showed that low-FIP elements increased more significantly than the high-FIP elements. A recent high-resolution X-ray spectroscopic study of a flare in HR 1099 with *XMM-Newton* showed a similar behavior (Audard, Güdel, & Mewe 2001b).

In this “electronic” paper, we present a study of abundances in RS CVn binary systems observed by *XMM-Newton*. In brief, it shows i) a transition from an inverse FIP effect to an absence of a FIP bias with decreasing activity, com-

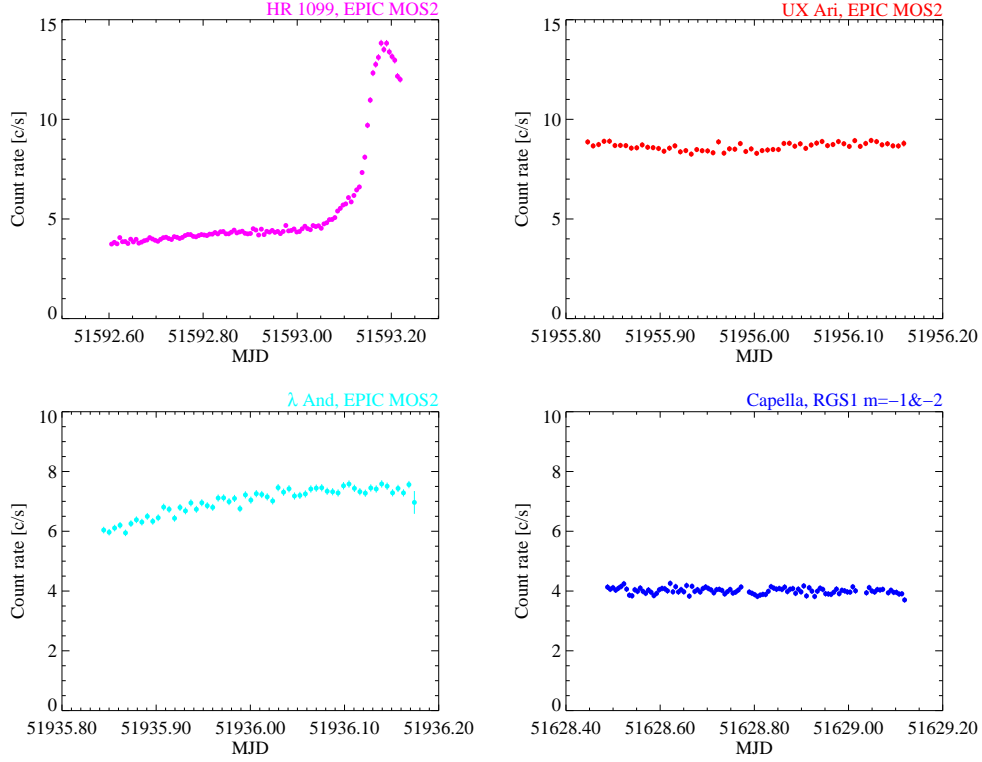


Figure 1. X-ray light curves of HR 1099, UX Ari,  $\lambda$  And, and Capella binned at 500 s. EPIC MOS2 light curves are shown, except for Capella where the sum of the RGS1 first and second order light curves is given, due to substantial pile-up and optical contamination of the EPIC data. Note that the EPIC count rate for HR 1099 is smaller as we had to use an annulus extraction region to account for pile-up in the central part of the PSF. Also, note that only the quiescent part of HR 1099 has been included in the analysis; see Fig. 6 for the flare analysis (also Audard et al. 2001b).

patible with a similar transition observed in solar analogs (Güdel et al. 2002; also in these proceedings), ii) a depletion of low-FIP elemental coronal abundances with increasing average coronal temperature, while high-FIP elemental abundances stay constant, iii) an enhancement of low-FIP elemental abundances during flares, while high-FIP elemental abundances again stay constant.

## 2. Observations and Data Analysis

*XMM-Newton* observed a number of RS CVn binary systems as part of the RGS stellar Guaranteed Time Program (see Güdel et al. in these proceedings). Here, we present an analysis of the quiescent observations of HR 1099, UX Ari,  $\lambda$  And, and Capella. Their light curves are shown in Figure 1 and their high-resolution

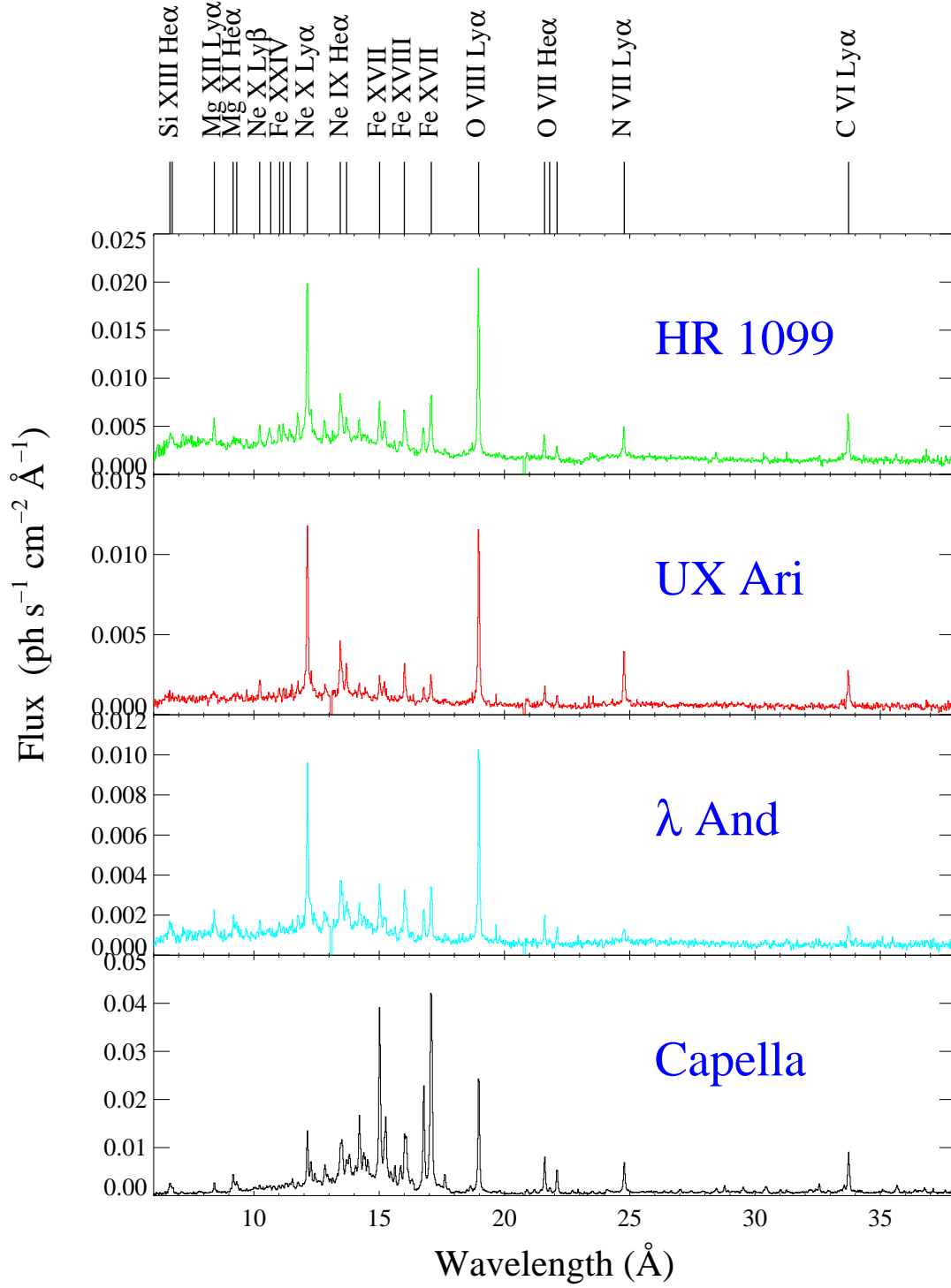


Figure 2. Fluxed *XMM-Newton* RGS spectra with some line identifications. The spectra are binned to a resolution of 25 m $\text{\AA}$ .

RGS spectra in Figure 2. The RGS1, RGS2, and EPIC MOS2 spectra (except for Capella where no EPIC data are available) were fitted simultaneously in XSPEC 11.0.1aj (Arnaud 1996) with the *vappec* model. We have removed significant parts of the RGS spectra above 20 Å to take into account the incompleteness and inaccuracy of the atomic database for non-Fe L-shell transitions. Additionally, some Fe L-shell lines with inaccurate atomic data were not fitted. A free multiplicative constant model has been introduced for cross-calibration uncertainties, finite extraction region and, in the case of HR 1099, an annulus-shaped extraction region. Notice that RGS1 and RGS2 each suffer from the loss of one CCD, but the combined spectra cover the whole RGS wavelength range (den Herder et al. 2001). Here we present results from fits on a grid of 10 components with fixed T, but free EM and abundances (the latter linked between the components).

### 3. Results

Figure 3 shows the coronal abundances normalized to the O abundance in order to ease comparison between the different stars. We used the solar photospheric abundances from Anders & Grevesse (1989), except for the Fe abundance which was taken from Grevesse & Sauval (1999). The panels are ordered in decreasing activity from top to bottom. Clearly, ratios for high-FIP elements exceed the ratios for low-FIP elements in very active stars (HR 1099, UX Ari), while for the less active, not tidally locked  $\lambda$  And, a poor correlation is observed. In the intermediately active Capella, no FIP bias is present although a possible weak FIP effect could be suggested. However, any bias is definitive only if coronal abundances of stars are compared to their respective photospheric abundances rather than to the solar values. Unfortunately, few photospheric abundances are known for RS CVn binaries.  $\lambda$  And is an exception: we have used the abundances derived by Donati, Henry, & Hall (1995) to normalize our coronal abundances (Fig. 4). Again, no clear correlation can be observed. Such a procedure needs to be applied to stars that do show a clear IFIP bias when normalized to solar photospheric values. New accurate measurements of photospheric abundances in these objects are timely.

The “average” temperature of a stellar corona is an indicator of activity that is defined here as  $\log \langle T \rangle = (\sum_i \log T_i \times EM_i) / (\sum_i EM_i)$ , where  $T_i$  and  $EM_i$  are the 10-T model temperatures and emission measures, respectively. We present samples of the abundance ratios relative to O (for the low-FIP Fe and the high-FIP Ne) as a function of  $\langle T \rangle$  (Fig. 5). Data points from solar analogs (Güdel et al. 2002; in these proceedings) have been added; the panels show a very different behavior: while the Fe/O ratios exponentially decrease with increasing temperature, the Ne/O ratios show no correlation with the average coronal temperature. Similar behavior is observed in other low-FIP and high-FIP elements, respectively.

While the preceding results are valid for a quiescent state, previous data showed that the average metallicity Z or the Fe abundance can increase during large flares. Medium spectral resolution observations with *ASCA* allowed Güdel et al. (1999) to obtain time-dependent measurements of several elemental abundances during a large flare in UX Ari. They found that low-FIP el-

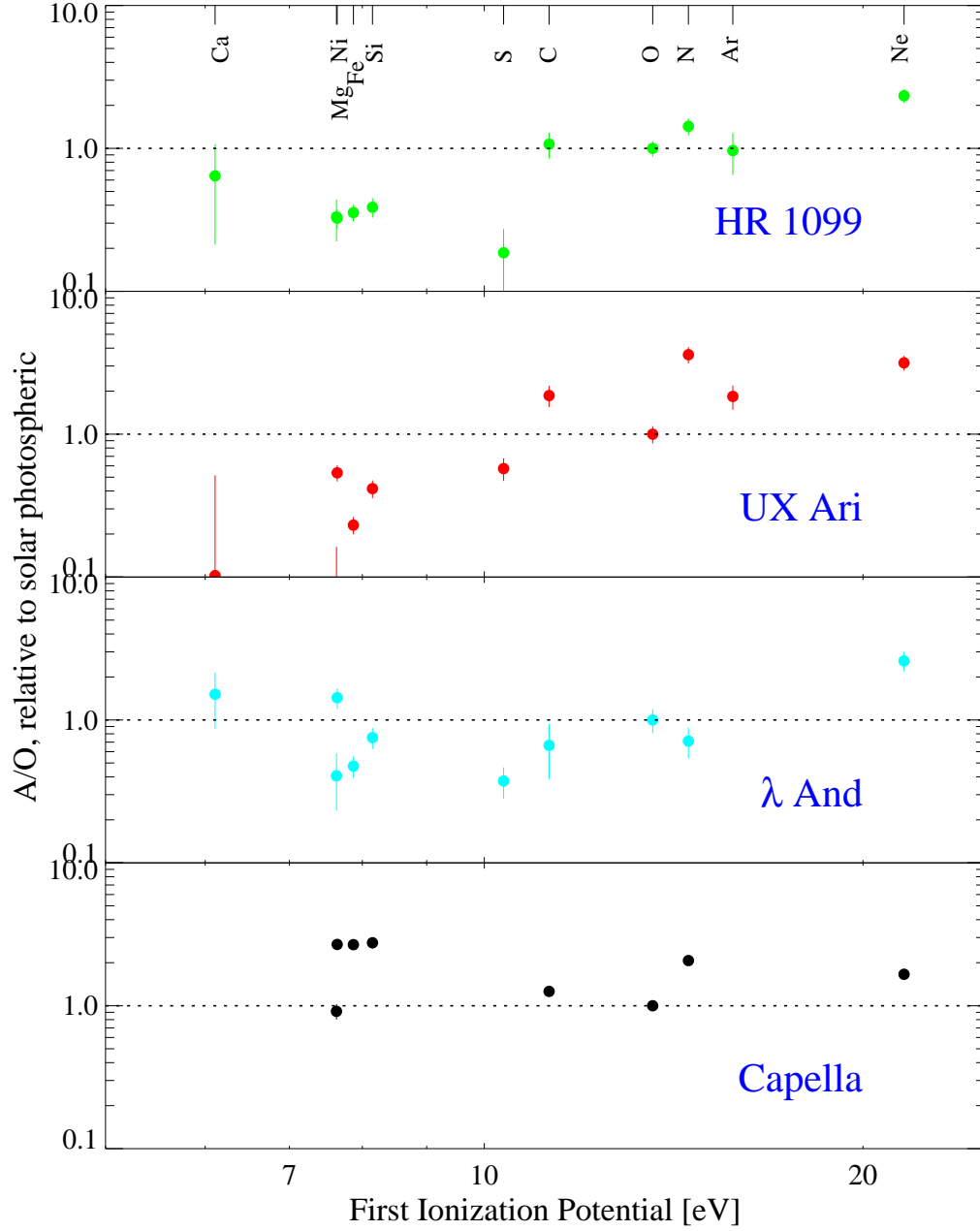


Figure 3. Coronal abundance ratios in RS CVn binaries as a function of the First Ionization Potential. The abundances have been normalized to O to allow for comparison. We used solar photospheric abundances from Anders & Grevesse (1989), except for Fe (Grevesse & Sauval 1999).

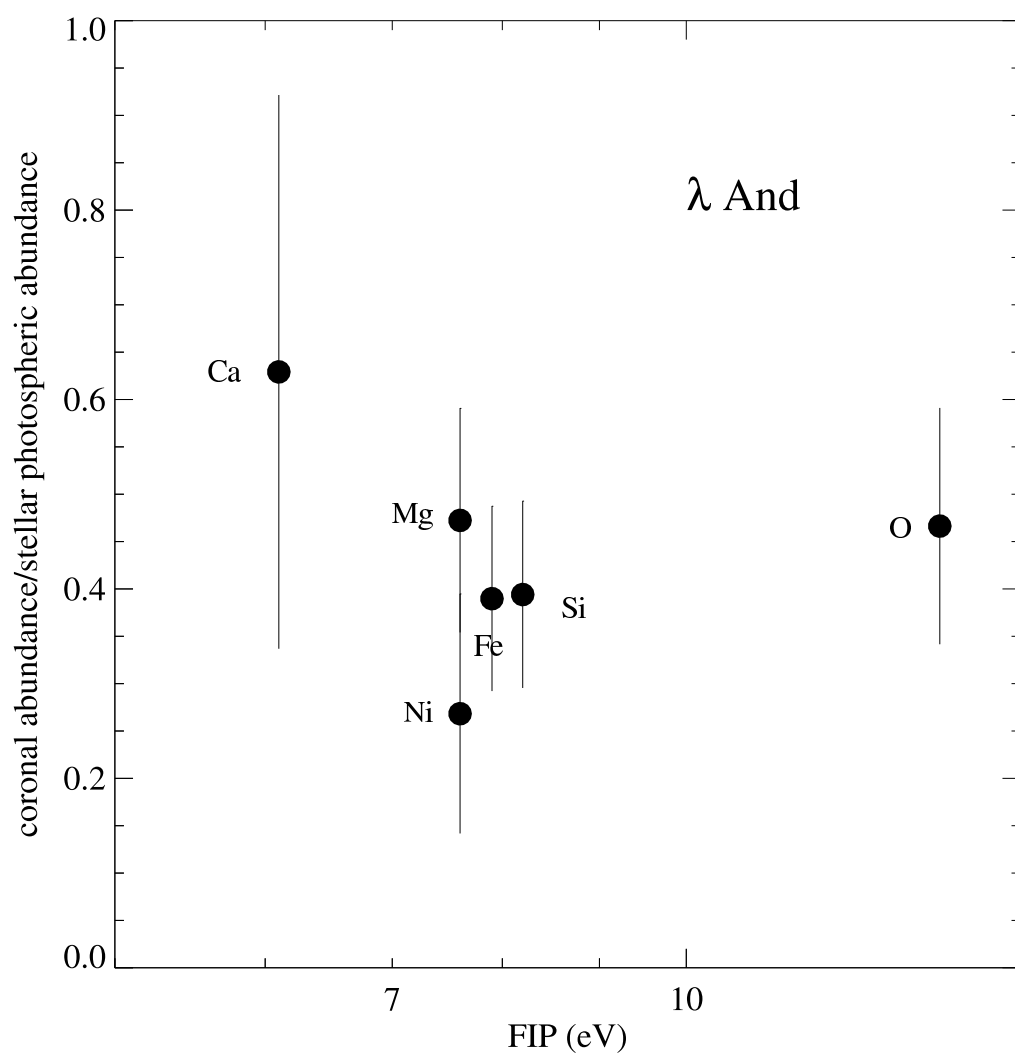


Figure 4. Coronal abundances of the RS CVn binary  $\lambda$  And relative to *stellar* photospheric abundances (Donati et al. 1995) as a function of FIP.

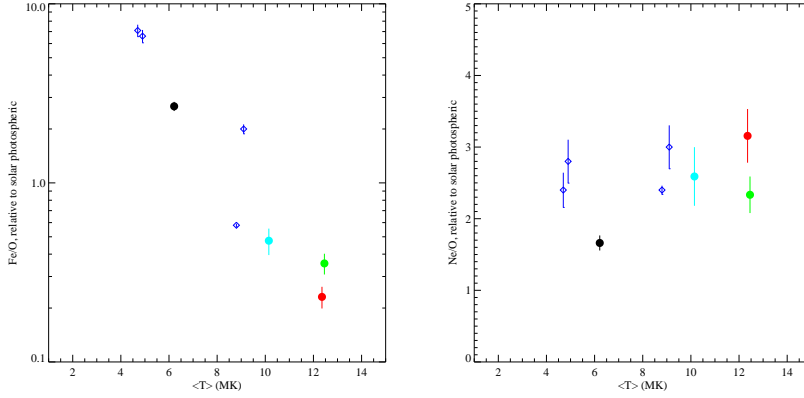


Figure 5. Coronal abundance ratio as a function of  $\langle T \rangle$ . *Left*: Fe/O ratios relative to solar photospheric for RS CVn binary systems (dots) with similar ratios for solar analogs (open diamonds, from Güdel et al. 2002; these proceedings). Note the logarithmic vertical scale. *Right*: Similar but for Ne/O ratios.

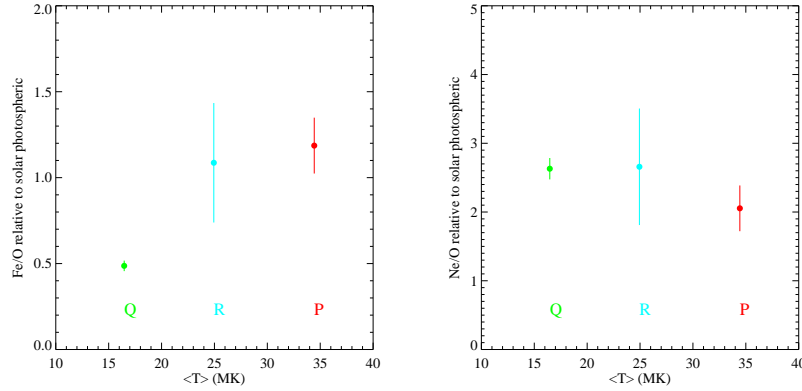


Figure 6. Coronal abundance ratio as a function of  $\langle T \rangle$  during a large flare in HR 1099. Left panel give Fe/O ratios, while the right panel gives Ne/O ratios. ‘Q’ stands for quiescent, ‘R’ for flare rise, and ‘P’ for flare peak.

elements increased more significantly than the high-FIP elements, although the latter could not be well-constrained due to blending (Ne) or low signal (Ar). A similar behavior was observed with recent *XMM-Newton* data of a flare in HR 1099 (Audard et al. 2001b). Here we present results of a reanalysis of this flare applying a more recent calibration. Figure 6 shows the Fe/O and Ne/O ratios as a function of the average temperature during quiescence, flare rise, and flare peak.

Consistent with the previous analysis (Audard et al. 2001b) and with previous results from other observations, the absolute Fe abundance increases during



the rising phase of the flare; however, the absolute Ne abundance stays constant. The Fe/O ratio also increases, while Ne/O remains constant, consistent with low-FIP elements being enhanced during flares while high-FIP elements staying equally abundant. Other low-FIP elements and high-FIP elements show similar respective behaviors.

#### 4. Discussion and Conclusion

We have found a correlation between the coronal elemental composition in active stars and the level of magnetic activity. The very active RS CVn binary systems show a clear trend toward an enhancement of coronal abundances of high-FIP elements (e.g., C, N, O, Ne) relative to low-FIP elements (e.g., Fe, Mg, Si). It is interpreted as a further evidence for an “Inverse First Ionization Potential” effect as found by Brinkman et al. (2001) in a deep exposure of HR 1099. Our sample (HR 1099, UX Ari,  $\lambda$  And, and Capella) covers high to intermediate magnetic activity levels. The most active stars show a clear IFIP effect, while the intermediately Capella show either an absence of a FIP bias or a weak FIP effect (Fig. 3). Using the average coronal temperature as an activity indicator, we find that coronal abundances of low-FIP elements (normalized to O) decrease with increasing temperature, while they stay constant for high-FIP elements. Note that such behavior will change if abundances are normalized to a low-FIP element such Fe. However, abundances relative to H suggest that low-FIP elemental abundances do vary with the level of magnetic activity, while this is not the case for high-FIP elements.

Our results agree well with the long-term evolution from an inverse FIP effect to a “normal” FIP effect found in solar analogs of solar photospheric composition (Güdel et al. 2002; these proceedings). Unfortunately, photospheric abundances are unknown for most RS CVn binary systems, and if known, measurements are largely scattered because it is difficult to obtain reliable photospheric abundances from optical spectroscopy, mainly because of enhanced chromospheric activity, high rotation velocities, and the presence of spots. Our target  $\lambda$  And is one of the rare cases with several measured photospheric abundances. Coronal abundances relative to the photospheric abundances derived by Donati et al. (1995) show no clear correlation with the FIP (Fig. 4). Accurate measurements of photospheric abundances in the most active stars are timely.

**Acknowledgments.** M. A. acknowledges support from the Swiss National Science Foundation (grant 2100-049343). He also thanks the organizers of the CS12 conference for financial support. The Space Research Organization of the Netherlands (SRON) is supported financially by NWO. This work is based on observations obtained with XMM-Newton, an ESA science mission with instruments and contributions directly funded by ESA Member States and the USA (NASA).

#### References

Anders, E., & Grevesse, N. 1989, *Geochim. Cosmochim. Acta*, 53, 197

- Arnaud, K. A. 1996, in ASP Conf. Ser. 101, *Astronomical Data Analysis Software and Systems V*, ed. G. Jacoby & J. Barnes (San Francisco: ASP), 17
- Audard, M., Behar, E., Güdel, M., et al. 2001a, *A&A*, 365, L329
- Audard, M., Güdel, M., & Mewe, R. 2001b, *A&A*, 365, L318
- Behar, E., Cottam, J., & Kahn, S. M. 2001, *ApJ*, 548, 966B
- Brinkman, A. C., Behar, E., Güdel, M., et al. 2001, *A&A*, 365, L324
- Dempsey, R. C., Linsky, J. L., Fleming, T. A., Schmitt, J. H. M. M. 1993, *ApJS*, 86, 599
- Donati, J.-F., Henry, G. W., & Hall, D. S. 1995, *A&A*, 293, 107
- Drake, J. J., Laming, J. M., & Widing, K. G. 1995, *ApJ*, 443, 393
- Drake, J. J., Laming, J. M., & Widing, K. G. 1997, *ApJ*, 478, 403
- Drake, S. A. 1996, in *Proceedings of the 6th Annual October Astrophysics Conference in College Park*, eds. S. S. Holt & G. Sonneborn, (San Francisco: ASP), 215
- Favata, F., Reale, F., Micela, G., Sciortino, S., Maggio, A., & Matsumoto, H. 2000, *A&A*, 353, 987
- Grevesse, N., & Sauval, A. J. 1999, *A&A*, 347, 348
- Güdel, M., Audard, M., Briggs, K., et al. 2001a, *A&A*, 365, L336
- Güdel, M., Audard, M., Magee, H., et al. 2001b, *A&A*, 365, L344
- Güdel, M., Audard, M., Sres, A., Wehrli, R., & Mewe, R. 2001c, *ApJ*, submitted
- Güdel, M., Linsky, J. L., Brown, A., & Nagase, F. 1999, *ApJ*, 511, 405
- Haisch, B., Saba, J. L. R., & Meyer, J.-P. 1996, in *IAU Colloquium 152, Astrophysics in the extreme ultraviolet*, ed. S. Boweyer & R. F. Malina (Dordrecht: Kluwer), 511
- Hall, D. S. 1976, in *IAU Colloquium 29, Multiple Period Variable Stars*, ed. W. S. Fitch (Dordrecht: Reidel), 287
- den Herder, J. W., Brinkman, A. C., Kahn, S. M., et al. 2001, *A&A*, 365, L7
- Laming, J. M., Drake, J. J., & Widing, K. G. 1996, *ApJ*, 462, 948
- Ottmann, R., & Schmitt, J. H. M. M. 1996, *A&A*, 307, 813
- Noyes, R. W., Hartmann, L. W., Baliunas, S. L., Duncan, D. K., & Vaughan, A. H. 1984, *ApJ*, 279, 763
- Schmitt, J. H. M. M., Stern, R. A., Drake, J. J., & Kürster, M. 1996, *ApJ*, 464, 898